

## Fingerprints of Reflection Asymmetry at High Angular Momentum in Atomic Nuclei

E. Garrote, J. L. Egidio, and L. M. Robledo

*Departamento de Física Teórica C-XI, Universidad Autónoma de Madrid, E-28049 Madrid, Spain*

(Received 28 October 1997; revised manuscript received 9 March 1998)

The reflection asymmetric phase transition in nuclei at high angular momentum is analyzed in the framework of the cranked Hartree-Fock-Bogoliubov approximation, with the Gogny interaction, using approximate parity projection before variation. The  $N = 88$  isotones are studied and our results compared with experimental data. Good agreement is found for the energy splitting of the even and odd parity states and  $B(E1)$  transition probabilities. Differences on intrinsic deformations, dipole moments, and pairing energies between odd and even parity states found at low spin disappear with increasing angular momentum. [S0031-9007(98)06128-6]

PACS numbers: 21.60.Jz, 21.10.Ky, 21.10.Re, 27.60.+j

The spontaneous symmetry breaking mechanism is associated with the appearance of collective phenomena and it has been a long studied subject in particular in atomic nuclei [1]. Quadrupole deformation and superfluidity are the best known. In atomic nuclei the most difficult to be measured has been, probably, the one associated with the breaking of the reflection symmetry, i.e., the spatial parity. Only recently there has been enough experimental data to draw some definitive conclusions.

In the last few years there have been many investigations devoted to the study of reflection asymmetry in nuclei; see Refs. [2,3] for recent reviews. The main features of octupole deformed nuclei are reflection asymmetry (pearlike shape) and “quasimolecular” rotational bands of alternating-parity states connected by strong electric-dipole transitions. Most experimental studies have been done at low angular momentum and only in recent years have there been measurements of higher-lying members of rotational bands in transitional and deformed nuclei [4–12] where the quasimolecular rotational bands are clearly observed.

From the theoretical point of view, several macroscopic [13–15] and microscopic [16–21] approximations have been developed to explain the experimental data. So far, most of the microscopic investigations have dealt with the ground state of even-even nuclei, but not much has been done for high spin states. The study of octupole correlations with microscopic self-consistent theories and effective forces at high angular momentum is very challenging because it makes parameter-free predictions and interpretations of experimental data.

To analyze the octupole degree of freedom at high spins, we have extended [22] our treatment of angular momentum constrained Hartree-Fock-Bogoliubov (CHFB) theory with the Gogny force [23] to include reflection asymmetric wave functions (w.f.). To compare with the experimental data, parity symmetry was restored in a *projection after variation* (PAV) approach: The unprojected energy is first minimized to determine the intrinsic w.f. and then the projected energy is computed using this intrinsic w.f. In the presence of octupole instabili-

ties this approximation is not the optimal one, because the negative parity states usually have a different octupole deformation than the positive parity ones. This possibility, obviously, cannot be considered in a PAV approach and in this approximation we are not able [22] to reproduce the experimental splittings. The *projection before variation* (PBV) method, however, allows different intrinsic w.f. for positive and negative parity states. The ansatz for a PBV w.f. of parity  $p$  and angular momentum  $I$  is given by

$$|\psi_p^I\rangle = \hat{P}_p |\phi^I\rangle, \quad \hat{P}_p = \frac{1}{2}(1 + p\hat{\Pi}) \quad (1)$$

with  $\hat{P}_p$  the parity projector,  $p = \pm$ ,  $\hat{\Pi}$  the standard parity operator [24], and  $|\phi^I\rangle$  the intrinsic, parity violating, w.f. to be determined by minimizing the projected energy.

In this Letter, as an approximation to *parity projection before variation* at high spin, we first determine the intrinsic w.f.  $|\phi^I(q_3)\rangle$  for a given angular momentum  $I$  by minimizing the  $q_3$ -constrained energy (see below). We then construct the projected w.f. of Eq. (1) and compute the projected energies as a function of  $q_3$ . The minimum of the projected energies provides the optimal intrinsic w.f. for a given spin and parity. By projection onto parity one can compute energy splittings and  $B(E1)$  transition probabilities as a function of the angular momentum. This approach allows us to investigate the fingerprints of a phase transition to octupole deformation driven by the angular momentum. This approach has already been used at zero angular momentum [24], and provides a very good approximation to the full PBV [25] method.

The interaction used in the calculations is the finite range density dependent Gogny force D1S [26]. The finite range of this force is very important for describing the pairing correlations. This interaction has been very successful in the description of many properties of spherical and deformed nuclei over the periodic table, and in particular the octupole properties of nuclei at zero angular momentum [17,20,24]. As an application of the method we study the experimentally measured high spin states of the  $N = 88$  isotones.

The simplest way to determine the intrinsic, octupole deformed, w.f.  $|\phi^I(q_3)\rangle$  is to use an unrestricted mean field variation. By unrestricted we mean that in the minimization of the energy we allow Hartree-Fock-Bogoliubov (HFB) w.f. which are not eigenstates of the symmetry operators  $\hat{N}$ ,  $\hat{\Pi}$ , etc., enlarging thereby the allowed variational Hilbert space. Within the HFB approach one deals with the symmetries, on the average, by introducing appropriate Lagrange multipliers.

The most general parity breaking Bogoliubov transformation is

$$\alpha_k^+ = \sum_l U_{lk} c_l^+ + V_{lk} c_l, \quad (2)$$

where  $c_l$  are the particle operators and the index  $l$  runs over states of positive and negative parity. The main consequence is that the HFB equation is not block diagonal in the four channels ( $\pi^+$ ,  $\pi^-$ ,  $\nu^+$ ,  $\nu^-$ ), but only in ( $\pi$ ,  $\nu$ ). As basis states we use those of the triaxial harmonic oscillator. In the present calculations, we use ten deformed [22] oscillator shells.

The HFB w.f.  $|\phi^I\rangle$  of Eq. (1), the vacuum of the quasiparticle operators  $\alpha_k$ , is obtained by the variational principle

$$\delta\langle\phi^I|\hat{H} - \lambda_i\hat{N}_i - \omega\hat{J}_x - \lambda_1\hat{Q}_{10} - \lambda_3\hat{Q}_{30}|\phi^I\rangle = 0. \quad (3)$$

The Lagrange multipliers are determined by the constraints  $\langle\phi^I|\hat{N}_i|\phi^I\rangle = N_i$ ,  $\langle\phi^I|\hat{J}_x|\phi^I\rangle = \sqrt{I(I+1)}$ ,  $\langle\phi^I|\hat{Q}_{10}|\phi^I\rangle = 0$ , and  $\langle\phi^I|\hat{Q}_{30}|\phi^I\rangle = q_3$ , with  $i = \pi, \nu$ . Since the parity symmetry is broken, it is necessary to constrain the mass dipole operator,  $\hat{Q}_{10}$ , to fix the position of the center of mass coordinate at the origin to decouple the spurious states. The constraint on the mass octupole operator,  $\hat{Q}_{30}$ , is used to fix the octupole moment at the desired  $q_3$  value. The w.f.  $|\phi^I\rangle$  determined in this way is a function of  $q_3$ , i.e.,  $|\phi^I(q_3)\rangle$ , and so is the projected one  $|\psi_p^I(q_3)\rangle$ . (Notice that  $q_3$  in the projected w.f. is merely used to label the w.f. Obviously, the expectation value of  $\hat{Q}_{30}$  with the projected w.f. is zero.) To describe a rotational band, the CHF equation (3) is solved for spin  $I = 0, 1, 2, 3, 4, \dots$  and different  $q_3$  values. The corresponding w.f.  $|\phi^I(q_3)\rangle$  are parity mixed. To get the splitting (if any) between the positive parity band ( $I = 0^+, 2^+, 4^+, \dots$ ) and the negative parity one ( $I = 1^-, 3^-, 5^-, \dots$ ), we project at states of good parity. As mentioned above, as an approximation to PBV, we calculate the projected energies

$$E_p^I(q_3) = \frac{\langle\psi_p^I(q_3)|\hat{H}|\psi_p^I(q_3)\rangle}{\langle\psi_p^I(q_3)|\psi_p^I(q_3)\rangle} \quad (4)$$

to find the minimum of  $E_p^I(q_3)$  as a function of  $q_3$ . Since the Gogny force is a functional of the density, in the evaluation of the projected energy one has to provide a prescription for the density dependence of the

Hamiltonian. In the present calculations, we use the same as in [24].

Once we know the projected w.f. we can calculate expectation values and transition matrix elements. To evaluate transition matrix elements we should, in principle, project onto good angular momentum. This is very complicated and we shall calculate them in the Kamlah approximation [27] to angular momentum projection.

As an example of our results, we show in Fig. 1 the CHF and projected [Eq. (4)] energies of the nucleus  $^{144}\text{Ba}$  for several spin values. At low  $I$ , the even parity states have an energy minimum at a lower intrinsic octupole moment than the odd parity states. At high  $I$ , however, both the even and odd parity states have their minima at the same value of the intrinsic octupole moment.

In Fig. 2 we show the deformation parameters  $\beta_2$ ,  $\beta_3$ ,  $\beta_4$ , pairing energies, and dipole moments  $D_0$ , calculated with the intrinsic wave functions at the energy minima of Fig. 1. Here the  $\beta_\lambda$  parameters are the deformation parameter of the liquid drop model with a sharp surface. All parameters show a staggering between odd and even- $I$

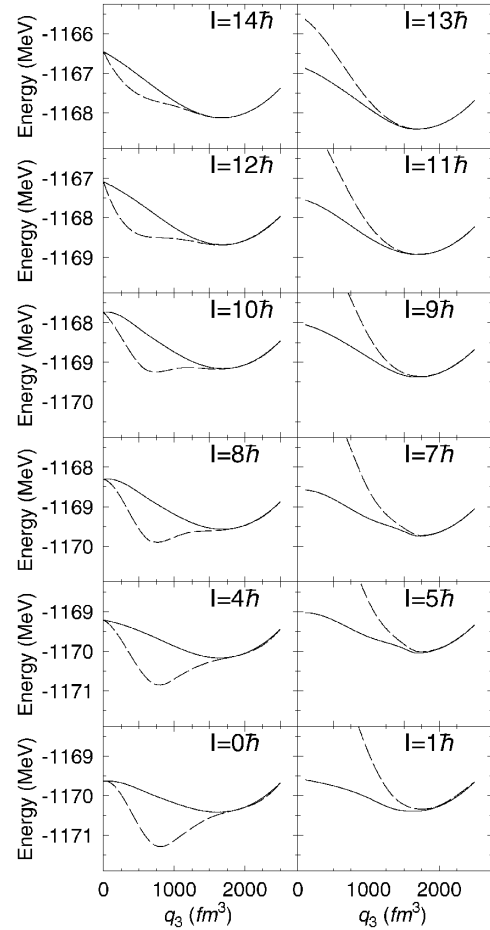


FIG. 1. Projected (dashed lines) and unprojected (solid lines) energies for  $^{144}\text{Ba}$  versus the octupole moment of the intrinsic w.f. Only natural parity projected energies are shown.

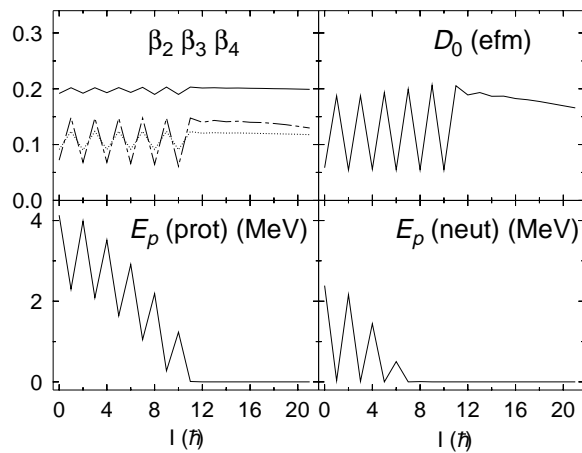


FIG. 2. Upper panel: Deformation parameters along the Yrast line for  $^{144}\text{Ba}$ ,  $\beta_2$  (solid line),  $\beta_3$  (dash-dotted line), and  $\beta_4$  (dotted line). Lower panel: Pairing energies for protons and neutrons for the same nucleus.

values at low angular momentum. At low spins, even- $I$  states have dipole moments roughly equal to 0.054 while the odd- $I$  have 0.187. At high  $I$ , the value of the dipole moment is approximately equal to 0.18 for both odd and even  $I$ . The experimental values for the dipole moment in  $^{144}\text{Ba}$  show a similar behavior, at  $I = 7$  the dipole moment is 0.07(10) and for  $I = 8-11$  is 0.14(3). This staggering is due to the fact that the intrinsic w.f. is different for even and odd- $I$  values. *It is interesting to notice that at high- $I$  values the staggering disappears, as one would expect in a phase transition from an octupole vibration to an octupole deformation.* The results for the other  $N = 88$  isotones are similar to the ones displayed for  $^{144}\text{Ba}$ .

The minima of the projected energies of Fig. 1 as a function of  $I$  determine the yrast states of positive and negative parity. Since the projected w.f. of Eq. (1) do not satisfy exactly the constraints on particle number and spin imposed on the intrinsic w.f., we correct for this in first order perturbation theory. In Fig. 3 we show the yrast bands of the  $N = 88$  isotones. As can be seen, the theoretical predictions are in excellent agreement with the experimental data. The common characteristic is the interleaving of different parity states at high angular momentum. This is the main characteristic of a rotational band in a octupole deformed nucleus. In  $^{144}\text{Ba}$ , for instance, the splitting at low spin is around 0.7 MeV. It decreases with growing spin up to  $I \sim 9\hbar$  where it vanishes. The situation is similar in the other nuclei.

In addition to the deformation parameters and the interleaving of the members of a rotational band, the strength of  $E1$  transitions between members of alternating parity bands is another significant observable of octupole deformed nuclei. They exhibit  $E1$  rates which are about 2 orders of magnitude faster than for reflection-symmetric nuclei. In Fig. 4 we display the  $B(E1)$  values as a function of the spin.

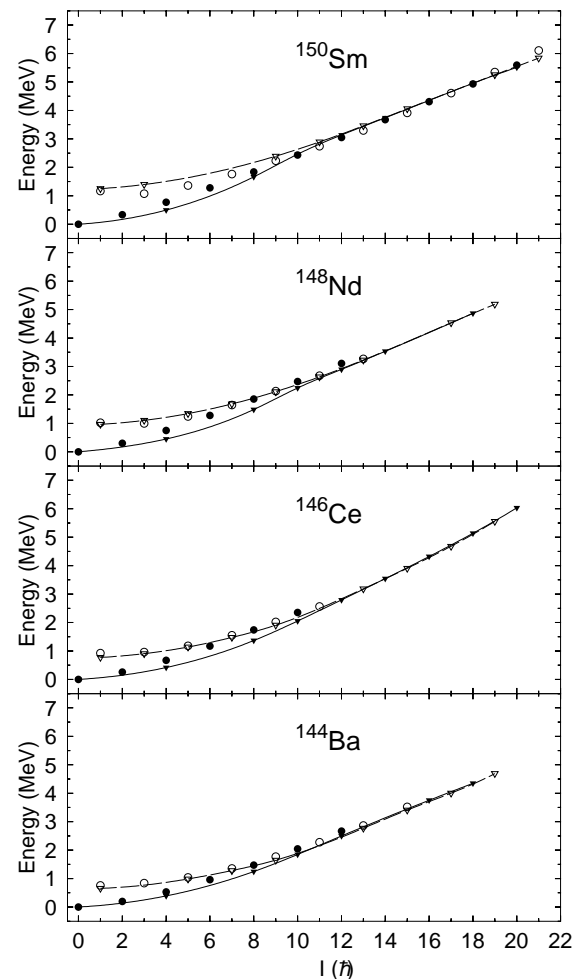


FIG. 3. Yrast lines of the  $N = 88$  isotones, for even (full labels) and odd (open labels)  $I$  values. The experimental data  $^{144}\text{Ba}$  [4,8],  $^{146}\text{Ce}$  [5],  $^{148}\text{Nd}$  [10], and  $^{150}\text{Sm}$  [6] are represented by circles and the theoretical ones by triangles.

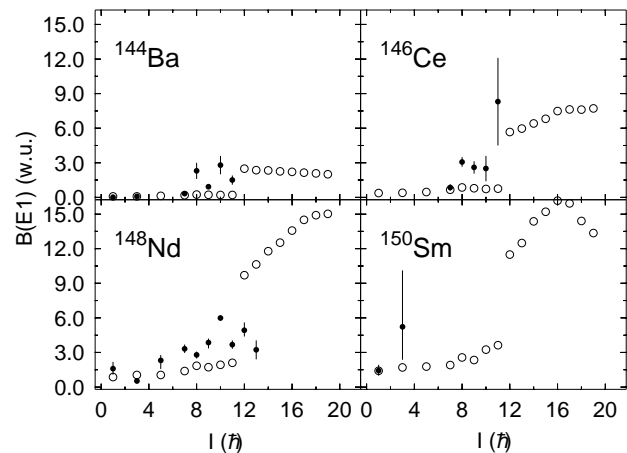


FIG. 4. Reduced transition probabilities  $E1$  of the  $N = 88$  isotones, versus the angular momentum. The experimental data  $^{144}\text{Ba}$  [4,9],  $^{146}\text{Ce}$  [5],  $^{148}\text{Nd}$  [10], and  $^{150}\text{Sm}$  [11] are represented by full circles and the theoretical results by open ones.

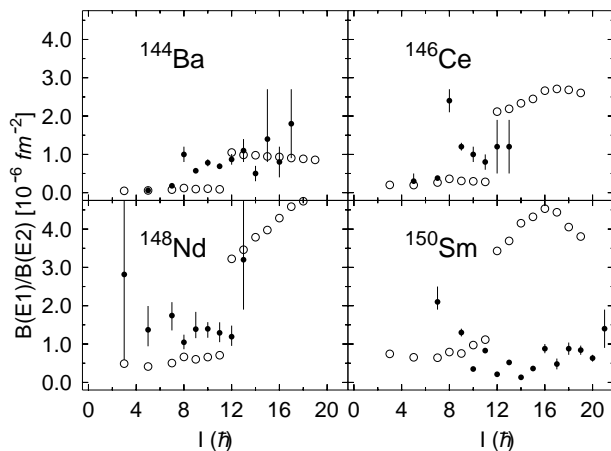


FIG. 5.  $B(E1)/B(E2)$  rates of the  $N = 88$  isotones versus the angular momentum. The experimental data  $^{144}\text{Ba}$  [8],  $^{146}\text{Ce}$  [12],  $^{148}\text{Nd}$  [7,10], and  $^{150}\text{Sm}$  [6,12] are represented by full circles and the theoretical results by open ones.

For spin values in the reflection-symmetric phase one expects smaller  $B(E1)$  values than in the reflection-asymmetric one (because of the poor w.f. matching of the initial and final states in the first case). In our calculations we get the phase transition around  $11\hbar$ ; at this spin value we find a jump in the  $B(E1)$  values. Experimentally the phase transition takes place around  $8\hbar$  and in  $^{144}\text{Ba}$  and  $^{146}\text{Ce}$  one can see the same enhancement in the  $B(E1)$ . In  $^{148}\text{Nd}$  the phase transition is not so pronounced (probably because  $^{148}\text{Nd}$  and  $^{150}\text{Sm}$  are transitional nuclei and shape fluctuations are important). In Fig. 5 we finally present the theoretical and experimental values of the  $B(E1)/B(E2)$  ratio. The agreement between theory and experiment is good for  $^{144}\text{Ba}$ ,  $^{146}\text{Ce}$ , and  $^{148}\text{Nd}$ . For  $^{150}\text{Sm}$  the agreement is not as good as for the other isotones because this nucleus is transitional and at high spin the shape fluctuations are very important [28]. These shape fluctuations are not considered in our approach; the experimental  $B(E2)$  values, therefore, are larger than the calculated ones and the  $B(E1)/B(E2)$  ratio accordingly smaller. We note that no effective charges have been used in the calculations and that the force parameters were adjusted many years ago.

In conclusion, for the first time, we have performed microscopic calculations of the yrast bands of heavy, octupole unstable nuclei with an approximate parity projection before the variation and parity-breaking cranked Hartree-Fock-Bogoliubov wave functions. The calculations have been performed with the finite range, density dependent Gogny force for the  $N = 88$  isotopes where experimental data were available. In particular we have evaluated the energy splitting of positive and negative parity states as well as projected transition probabilities. The

theoretical predictions are, in general, in very good agreement with the experimental ones. This is particularly notable as there was no adjustment of parameters in this calculation. Our results confirm the interpretation of a phase transition to octupole deformed nuclei at high spins for these nuclei.

This work was supported in part by DGICYT, Spain under Project No. PB94-0164. One of us (E. G.) acknowledges a Mutis grant from the Spanish Institute of Cooperation. We thank W. Urban for providing us with data prior to publication and to R. R. Chasman for a careful reading of the manuscript.

- [1] A. Bohr and B. Mottelson, *Nuclear Structure* (Benjamin, New York, 1969).
- [2] I. Ahmad and P. A. Butler, *Annu. Rev. Nucl. Part. Sci.* **43**, 71 (1993).
- [3] P. A. Butler and W. Nazarewicz, *Rev. Mod. Phys.* **68**, 349 (1996).
- [4] W. R. Phillips *et al.*, *Phys. Rev. Lett.* **57**, 3257 (1986).
- [5] W. R. Phillips *et al.*, *Phys. Lett. B* **212**, 402 (1988).
- [6] W. Urban *et al.*, *Phys. Lett. B* **185**, 331 (1987).
- [7] W. Urban *et al.*, *Phys. Lett. B* **200**, 424 (1988).
- [8] W. Urban *et al.*, *Nucl. Phys.* **A613**, 107 (1997).
- [9] H. Mach *et al.*, *Phys. Rev. C* **41**, R2469 (1990).
- [10] R. Ibbotson *et al.*, *Phys. Rev. Lett.* **71**, 1990 (1993).
- [11] A. Jungclaus *et al.*, *Phys. Rev. C* **48**, 1005 (1993).
- [12] W. Urban (private communication).
- [13] W. Nazarewicz *et al.*, *Nucl. Phys.* **A429**, 269 (1984).
- [14] W. Nazarewicz *et al.*, *Phys. Rev. Lett.* **52**, 1272 (1984).
- [15] W. Nazarewicz and S. L. Tabor, *Phys. Rev. C* **45**, 2226 (1992).
- [16] P. Bonche, *The Variety of Nuclear Shapes*, edited by J. D. Garrett *et al.* (World Scientific, Singapore, 1989), p. 302.
- [17] L. M. Robledo, J. L. Egido, J. F. Berger, and M. Girod, *Phys. Lett. B* **187**, 223 (1987).
- [18] R. R. Chasman, *Phys. Lett.* **96B**, 7 (1980).
- [19] R. R. Chasman, *Phys. Lett. B* **219**, 232 (1989).
- [20] L. M. Robledo, J. L. Egido, B. Nerlo-Pomorska, and K. Pomorski, *Phys. Lett. B* **201**, 409 (1988).
- [21] P. Bonche *et al.*, *Phys. Rev. Lett.* **66**, 876 (1991).
- [22] E. Garrote, J. L. Egido, and L. M. Robledo, *Phys. Lett. B* **410**, 86 (1997).
- [23] J. L. Egido and L. M. Robledo, *Phys. Rev. Lett.* **70**, 2876 (1993).
- [24] J. L. Egido and L. M. Robledo, *Nucl. Phys.* **A524**, 65 (1991).
- [25] L. M. Robledo, *Phys. Rev. C* **46**, 238 (1992).
- [26] J. F. Berger, M. Girod, and D. Gogny, *Nucl. Phys.* **A428**, 23c (1984).
- [27] J. L. Egido and H. A. Weidemüller, *Phys. Rev. C* **39**, 2398 (1989).
- [28] J. Meyer, P. Bonche, M. S. Weisse, J. Dobaczewski, H. Flocard, and P. H. Heenen, *Nucl. Phys.* **A588**, 597 (1995).